THE JOURNAL OF BIOLOGICAL CHEMISTRY VOL. 291, NO. 33, pp. 17345–17359, August 12, 2016

Functional Diversity of Human Mitochondrial J-proteins Is Independent of Their Association with the Inner Membrane Presequence Translocase*[S]

Received for publication, May 13, 2016, and in revised form, June 16, 2016 Published, JBC Papers in Press, June 21, 2016, DOI 10.1074/jbc.M116.738146

Devanjan Sinha[1], **Shubhi Srivastava, and Patrick D'Silva**[2]

From the Department of Biochemistry, Indian Institute of Science, Bangalore 560012, Karnataka, India

Mitochondrial J-proteins play a critical role in governing Hsp70 activity and, hence, are essential for organellar protein translocation and folding. In contrast to yeast, which has a single J-protein Pam18, humans involve two J-proteins, DnaJC15 and DnaJC19, associated with contrasting cellular phenotype, to transport proteins into the mitochondria. Mutation in DnaJC19 results in dilated cardiomyopathy and ataxia syndrome, whereas expression of DnaJC15 regulates the response of cancer cells to chemotherapy. In the present study we have comparatively assessed the biochemical properties of the J-protein paralogs in relation to their association with the import channel. Both DnaJC15 and DnaJC19 formed two distinct subcomplexes with Magmas at the import channel. Knockdown analysis suggested an essential role for Magmas and DnaJC19 in organellar protein translocation and mitochondria biogenesis, whereas DnaJC15 had dispensable supportive function. The J-proteins were found to have equal affinity for Magmas and could stimulate mitochondrial Hsp70 ATPase activity by equivalent levels. Interestingly, we observed that DnaJC15 exhibits bifunctional properties. At the translocation channel, it involves conserved interactions and mechanism to translocate the precursors into mitochondria. In addition to protein transport, DnaJC15 also showed a dual role in yeast where its expression elicited enhanced sensitivity of cells to cisplatin that required the presence of a functional J-domain. The amount of DnaJC15 expressed in the cell was directly proportional to the sensitivity of cells. Our analysis indicates that the differential cellular phenotype displayed by human mitochondrial J-proteins is independent of their activity and association with Magmas at the translocation channel.

In eukaryotic cells mitochondria form an essential organelle that plays a central role in cancer, apoptosis, and cytotoxic responses and maintains the overall metabolic homeostasis within the cell (1, 2). More than 98% of the human mitochondrial protein pool is nuclear-encoded and transported into the mitochondria through highly complex import machinery spanning the outer membrane, inner membrane, and the intermembrane space (2, 3). At the inner membrane, TIM23 complex forms the sole gateway for translocation of precursor proteins into the matrix, which accounts for ~60% of the total imported proteins (4, 5). The TIM23 complex comprises of two components: membrane-embedded Tim23 core channel and the motor component. Although the initial membrane potential dependent translocation is mediated by the Tim23-Tim17 channel, it is the overall activity of the import motor, which determines the translocation process (3, 4, 6–10). The import motor contains mtHsp70 as its core, whose function is orchestrated by J-proteins (7, 11–13). The ADP/ATP states of Hsp70 regulate its interactions with client proteins (14, 15). However, the basal ATPase activity of Hsp70 is not sufficient to drive the reactions efficiently and, thus, requires J-proteins as cofactors to stimulate its ATPase activity (11, 16, 17). Hence, J-proteins are the critical components of the Hsp70 chaperone machine and drive the multifunctionality of Hsp70s (11).

In yeast, mitochondrial import motor consists of a single J-protein, Pam18, which stimulates yeast mitochondrial Hsp70 (Ssc1) ATPase activity. Pam18 forms a heterodimeric subcomplex with Pam16, a J-like protein that inhibits its ATPase stimulatory activity and thereby exerts a regulatory role on the overall activity of import motor and the transport process (12, 18–21). Homologs of Pam16 and Pam18-like proteins are found across all eukaryotic species. The ortholog of Pam16, identified in humans as Magmas, is essential for biogenesis of mitochondria and also plays an additional role in regulation of reactive oxygen species in humans (22). A recent observation showed Magmas to function as a ROS (reactive oxygen species) regulator where it maintains the cellular redox state under stress conditions by promoting efficient oxidative phosphorylation (OXPHOS) activity and enhanced reactive oxygen species scavenging (22). However, the primary function of Magmas remains strongly conserved. Magmas forms a part of the human import motor (23) and regulates the import process by inhibiting the human mtHsp70 (also known as Mortalin) ATPase stimulatory activity of its J-protein counterpart, DnaJC19 (JC19) (24). Recent reports suggest the presence of another member of DnaJ protein family DnaJC15 (JC15) in human mitochondria that may be potentially involved in the mitochondrial protein import process (25, 26). This is in contrast with the yeast system where the overall import process is governed by a single J-protein, Pam18 (27, 28). Both JC19 and JC15

* This work was supported by Swarnajayanti Fellowship, Department of Science and Technology (DST), India (to P. D. S), Council of Scientific and Industrial Research Fellowship (to D. S), and Department of Science and Technology INSPIRE Fellowship (to S. S). The authors declare that they have no conflicts of interest with the contents of this article.

[S] This article contains supplemental Figs. S1–S4.

[1] Present address: Dept. of Zoology, Institute of Science, Banaras Hindu University, Uttar Pradesh, Varanasi 221005, India.

[2] To whom correspondence should be addressed: Dept. of Biochemistry, Indian Institute of Science, Biological Sciences Bldg., Bangalore 560012, Karnataka, India. Tel.: 91-080-22932821; Fax: 91-080-23600814; E-mail: patrick@biochem.iisc.ernet.in.

are related to Pam18 in several aspects. Both have a significant sequence and structural similarity with its yeast ortholog. The C-terminal region of JC15 and JC19 consists of three helices similar to that of the Pam18 J-domain with a tightly packed canonical HPD motif between its helix II and helix III. Both localize into the mitochondria and are associated with the inner mitochondrial membrane via a single transmembrane helix with its J-domain facing the matrix side.

Interestingly, JC15 was first identified as a protein whose hypermethylation-mediated transcriptional silencing resulted in increased resistance to chemotherapeutic agents in ovarian carcinoma cells (29–32). The CpG island at the first exon of the *DNAJC15* gene was found to be methylated, and the number of methylated CpG sites in the island governs the extent of JC15 expression in the cancer cells and in normal tissues (29, 31). JC15 expression was found to decrease cellular survivability under xenobiotic stress conditions by modulating the opening of mitochondrial permeability transition pore complex through its association with cyclophilin D (33). Hence, it was suggested that loss of expression of JC15 contributes to the malignant phenotype by conferring resistance to various anti-cancer drugs by modulating the chemotherapeutic response of the cancer cells and served as a molecular marker for the response to chemotherapy (29, 31). Evidence also suggests JC15 to be a modulator of respiratory chain activity where it acts as an inhibitor of complex I (34). In contrast, a loss of function mutation in the J-domain of JC19 leads to a severe pathophysiological disorder, dilated cardiomyopathy and ataxia (DCM)[3] syndrome, that is characterized by cardiomyopathy and ataxia (24). It has been suggested that loss of subcomplex formation between JC19 and Magmas results in import defect and generation of characteristic DCM phenotypes (23, 24, 35).

Although much study has been done on the relationship of the J-proteins and cellular phenotype, no comparative information on the specificities of J-proteins is available. Here we show that unlike JC19, JC15 could complement growth of yeast cells deleted for *PAM18* and shows characteristics that are functionally similar to Pam18. In addition, JC15 was found to possess a conserved function of eliciting a chemosensitive response in yeast cells, which is indicative of its dual function in eukaryotic cell. We characterized the behavior of both the J-proteins in human cells, and our results indicate that the differential function of the two J-proteins is independent of their subcomplex formation with Magmas.

Results

Formation of Two Distinct Dimeric Subcomplexes between Magmas and J-proteins in Human Mitochondria—Primary observations have shown that components of the human TIM23 complex are conserved during evolution from yeast (23, 36). Human mtHsp70 forms the central component of the import motor along with hTim44 and Magmas. Magmas in turn forms a stable subcomplex with the third component JC19, which is the J-protein counterpart of mtHsp70. JC19 co-immunoprecipitates with Magmas and is tethered to the import complex by virtue of its interaction with Magmas (23, 37). Because JC15 is associated with the inner mitochondrial membrane in a manner similar to Pam18/JC19 and interacts with Magmas *in vitro* through its J-domain, we investigated the association of the three J-proteins in human mitochondria. To address, mitochondria from HEK293T cells were lysed using 1% Triton X-100 and subjected to co-immunoprecipitation (co-IP) analysis using antibodies specific to Magmas, JC19 or JC15. Interestingly, upon co-IP using anti-Magmas antibodies and subsequent immunodecoration by JC19- and JC15-specific antibodies, we observed pulldown of both JC19 and JC15 along with Magmas (Fig. 1*A*). This indicates that Magmas forms a subcomplex with both JC19 and JC15 in human mitochondria. On the other hand, reverse co-IP analysis using antibodies specific to the individual J-proteins resulted in different interesting observations. Immunoprecipitation using anti-JC19 antibodies resulted in a pulldown of Magmas along with JC19, and no co-immunoprecipitating band corresponding to JC15 was observed (Fig. 1*A*). Similarly, no co-IP of JC19 was detected when immunoprecipitation was performed using anti-JC15 antibodies; however, it resulted in the pulldown of Magmas along with JC15 (Fig. 1*A*). This shows that in human mitochondria, both J-proteins, JC19 and JC15, were able to form two distinct stable subcomplexes with Magmas.

To confirm that the formation of two J-protein subcomplexes at the import motor is independent of each other, mitochondria down-regulated for either Magmas, JC19, or JC15 (Fig. 1*B*), were subjected to co-immunoprecipitation analysis with anti-Magmas antibodies, and the association of respective J-proteins with Magmas was analyzed. We observed that depletion of Magmas caused abolition of both JC15 and JC19 subcomplexes, indicating the central role of Magmas in J-protein subcomplex formation at the import channel (Fig. 1*C*). However, down-regulation of JC19 did not affect subcomplex formation between Magmas and JC15, although JC19·Magmas subcomplex got abolished (Fig. 1*C*). Similarly, knockdown of JC15 resulted in abrogation of Magmas·JC15 but did not affect subcomplex formation between Magmas and JC19 (Fig. 1*C*). This indicated that subcomplexes formation between the J-proteins with that of Magmas is mutually exclusive of each other.

In the case of yeast, chromatographic methods and crystallographic analysis indicated the existence of self-oligomers of Pam16-Pam18 heteromers at the import motor (19). We ascertained the nature of subcomplex formation in human mitochondria through blue-native polyacrylamide gel electrophoresis (blue native-PAGE) and compared it with the yeast system. The oligomer formation under *in vivo* conditions was determined by comparing the basic heterodimeric subcomplexes isolated from Triton X-100-treated mitochondria with the undissociated complexes in digitonin-lysed mitochondria. It is known that in dissolution of mitochondria a stronger detergent treatment such as Triton X-100 disrupts comparatively weaker interactions between membrane proteins of the translocase. However, relatively stable interactions between the J-proteins dimers are well maintained. In contrast, a mild detergent treatment such as digitonin dissolves the intervening membranes

[3] The abbreviations used are: DCM, dilated cardiomyopathy and ataxia; dsiRNA, double-stranded small interfering RNA; co-IP, co-immunoprecipitation; NAO, *n*-nonyl acridine orange; DHFR, dihydrofolate reductase.

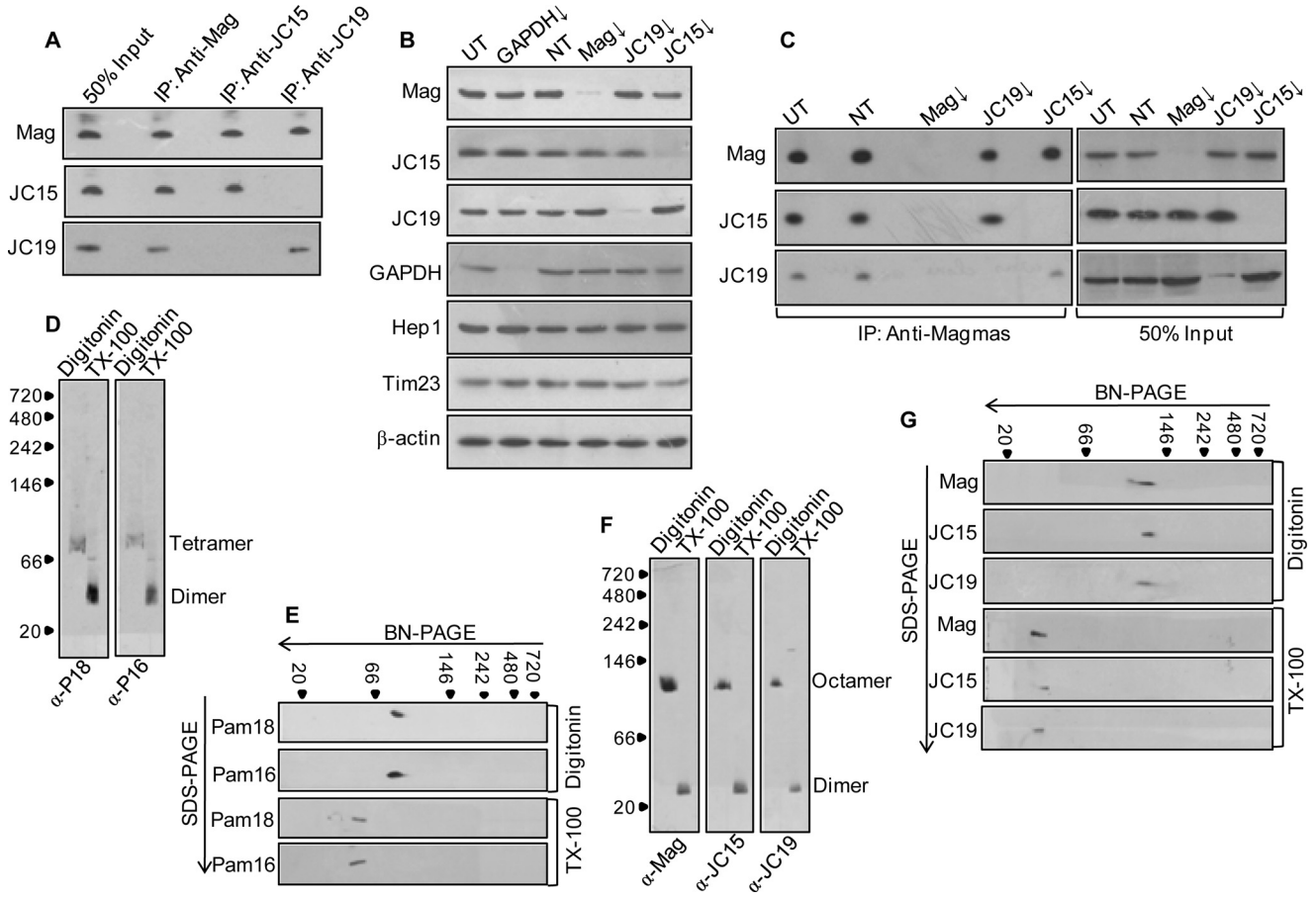

FIGURE 1. **Assembly of import motor associated J-protein subcomplexes at the translocation channel.** *A*, Triton X-100-lysed mitochondria were subjected to immunoprecipitation using anti-Magmas, anti-JC19, or anti-JC15 antibodies. The interacting proteins were probed by immunoblotting using specific antibodies. 50% of soluble material after lysis was used as the loading control (50% *Input*). *B*, HEK293T cells were seeded in Opti-MEM media and transfected with 5 μM siRNA pool against Magmas (*Mag*), JC19, and JC15 using Lipofectamine 2000. After 48 h, mitochondria were isolated and probed for expression of individual proteins. siGAPDH was used as a positive control, Hep1 was the mitochondrial loading control, β-actin was the initial cell concentration control, Tim23 was a control for translocase integrity. *C*, the assembly of J-protein subcomplex upon knockdown of individual protein components was assayed by subjecting the isolated mitochondria to co-immunoprecipitation analysis using anti-Magmas antibodies. The immunoprecipitates were separated on SDS-PAGE and probed with antibodies specific to Magmas, JC15, and JC19. 50% of the soluble material after lysis was used as a loading control (50% *Input*). *D* and *F*, 1% Triton X-100 or 1% digitonin-lysed human mitochondria was resolved on blue native gel and immunoblotted with Magmas-, JC19-, or JC15-specific antibodies. To decipher the oligomeric state, the relative migration of the bands was mapped onto the molecular weight standard. To correlate, equivalently treated yeast mitochondria (*D*) was subjected to blue native PAGE and immunoblotted with Pam16 or Pam18 antibodies. *E* and *G*, analysis of J-protein oligomerization through two-dimensional immunoblot of Triton X-100 (*TX-100*) and digitonin-lysed yeast (*E*) and human (*G*) mitochondria. Mitochondrial lysates were resolved on blue native (*BN-PAGE*) PAGE followed by second dimension separation on SDS-PAGE. Individual components of the oligomers were determined by staining the blot with respective antibodies. *UT*, untransfected control; *NT*, transfected with non-targeting dsiRNA as internal control; ↓, mRNA down-regulated by dsiRNA).

without affecting the association of the translocase components (19, 20, 27, 38). The isolated complexes can be resolved through blue native-PAGE and detected by immunoblotting. We found that resolution of yeast and human mitochondria subjected to differential detergent treatment, through blue native-PAGE, resulted in generation of two different profiles for yeast and humans, respectively. Intriguingly, under digitonin treatment JC15, JC19 and Magmas co-migrated as an octamer of 130–140-kDa size (Fig. 1*F*) compared with an ~80-kDa tetrameric state of yeast counterpart complex (Fig. 1*D*). On the other hand, in the presence of Triton X-100, the complexes migrated to heterodimer size of 30–35 kDa (Fig. 1*F*) as compared with ~40 kDa of the yeast system (Fig. 1*D*). This shows that in contrast to the yeast system, human J-proteins show significant organizational diversity and forms a higher order oligomeric structure at the translocase channel.

To rule out the possibility of higher order homodimeric forms of individual J-proteins, we performed a two-dimensional blue native-PAGE analysis, where the blue-native gels containing the higher order oligomeric and dimeric states of the J-protein subcomplexes were resolved through second-dimension SDS-PAGE immunoblot analysis. We observed that similar to the J-protein dimers, the oligomers also resolved into Magmas and JC19 or JC15, thereby indicating the existence of the subcomplexes as heterodimers (Fig. 1*G*). The findings were further verified in yeast mitochondria where the tetramers separated into Pam18 and Pam16 (Fig. 1*E*), proving the involvement of J-protein dimers in the oligomerization.

Essentiality of J-proteins for the Maintenance of Cell Viability and Mitochondrial Function—Our results indicate the association of two J-proteins with Magmas at the presequence translocase of the inner membrane. Based on this fact, we posed a

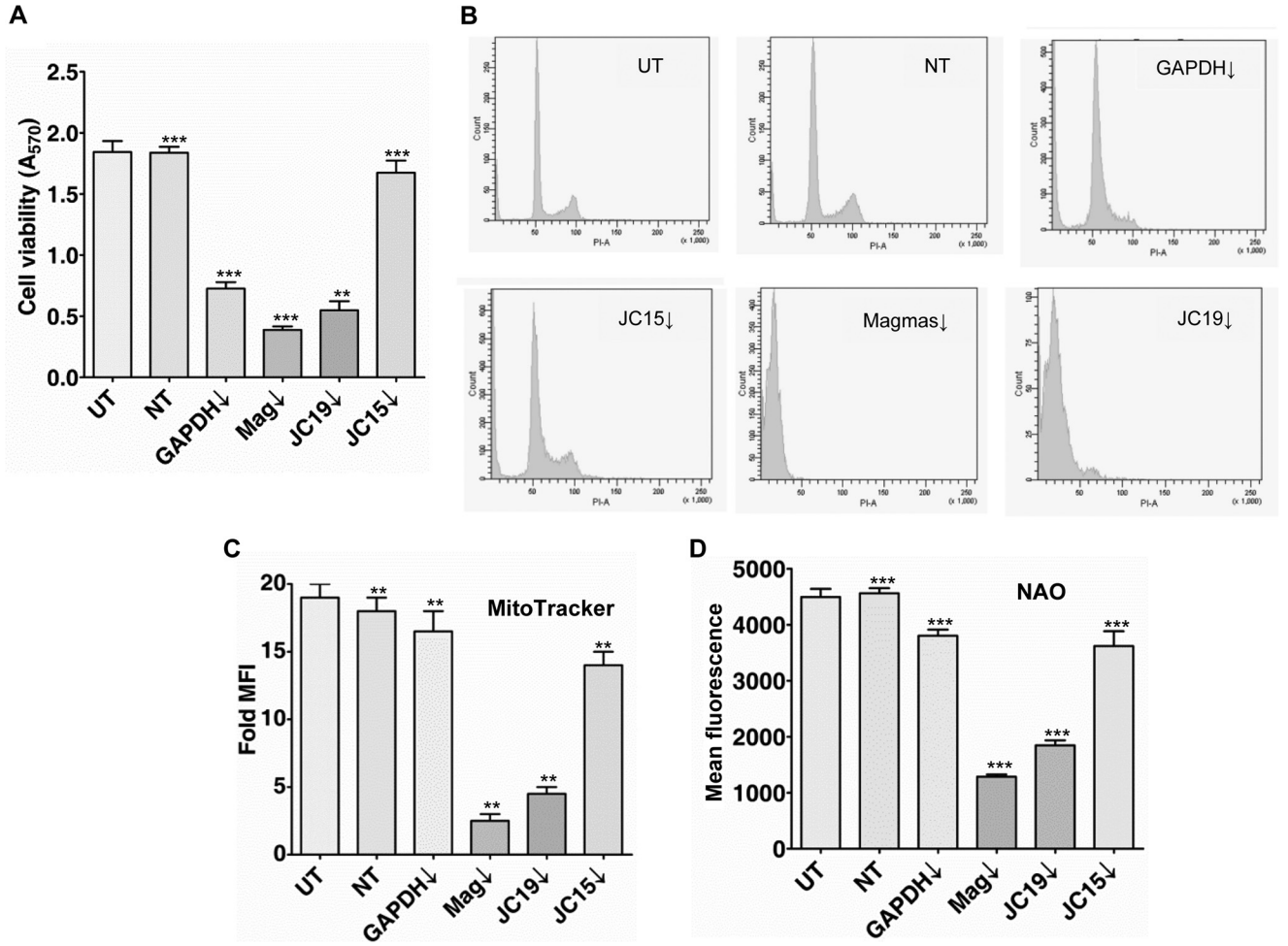

FIGURE 2. **Role of individual J-proteins in the maintenance of mitochondria biogenesis.** *A*, HEK293T cells were transfected with siRNA specific to the designated proteins and incubated for 48 h. Cell viability was determined through methyl thiazole tetrazolium (*MTT*) assay by detecting the amount of formazan formed at 540 nm. Data are represented as the mean ± S.E. $n = 8$; ***, p (two tailed) < 0.0001; **, p (two tailed) < 0.001. *B*, effect of Magmas and J-protein down-regulation on cell cycle progression. HEK293T cells transfected with siRNA pool against Magmas, JC15, and JC19 were harvested and fixed with 70% ethanol followed by RNase treatment. The cells were stained by propidium iodide and analyzed by flow cytometry. *C*, amount of functional mitochondria under down-regulated conditions was assessed by MitoTracker Deep Red staining. $n = 3$. **, p (two tailed) < 0.001. *D*, effect of altered expression of J-proteins on overall mitochondrial content was investigated by labeling the cells with NAO followed by flow cytometry analysis at $E_m = 535$ nm. The amount of fluorescence was directly correlated with mitochondrial content. $n = 3$. ***, p (two-tailed) < 0.0001. *UT*, untransfected control; *NT*, transfected with non-targeting dsiRNA as internal control. *MFI*, mean fluorescence intensity.

question on the criticality of either J-protein subcomplexes on the maintenance of normal mitochondrial function and cell growth. To test the *in vivo* critical functional attributes of the J- and J-like proteins in the human mitochondrial biogenesis, we performed siRNA-mediated knockdown analysis of Magmas, JC19, and JC15 and assessed the resultant phenotype. Down-regulation of Magmas and JC19 generated deleterious effects on cell viability as compared with JC15 depletion and untransfected control (Fig. 2*A*). Cells transfected with non-targeting siRNA served as the negative control, and viability of these cells was similar to unsilenced cells. The baseline cellular viability for unsilenced cells was found to be ~98–99% (data not shown). To further verify the role of each J-protein in maintenance of the cellular viability, silenced and unsilenced cells were subjected to cell-cycle analysis. We observed cells down-regulated for Magmas and JC19 showed increased accumulation of sub-G_1 population (Fig. 2*B*) as compared with untransfected cells, cells transfected with non-targeting siRNA, and JC15 knockdown cells, thus indicating that lowered level of Magmas and JC19 is associated with reduced cell viability. To rule out the possibility that the loss of cell viability due to reduced expression of Magmas and JC19 is a cell-specific phenomenon, we validated our findings by performing similar J-protein depletion experiments in a wide array of cell lines and assessed their viability. In line with our previous observation, down-regulation of Magmas and JC19 resulted in increased mortality of cells, whereas JC15 knockdown had a minimal effect on cell survivability (supplemental Fig. S1). In summary, Magmas and JC19 are essential for viability of cells, whereas JC15 is non-essential.

We further addressed whether the increase in cell mortality in case of Magmas and JC19 down-regulated cells is due to loss of mitochondrial function. First, we assessed the effect of J-proteins' down-regulation on the maintenance of mitochondria biogenesis by analyzing two parameters, namely, the amount of functional mitochondria and overall mitochondrial content (26). We found that down-regulation of Magmas and JC19 caused significant reduction in amount of functional mito-

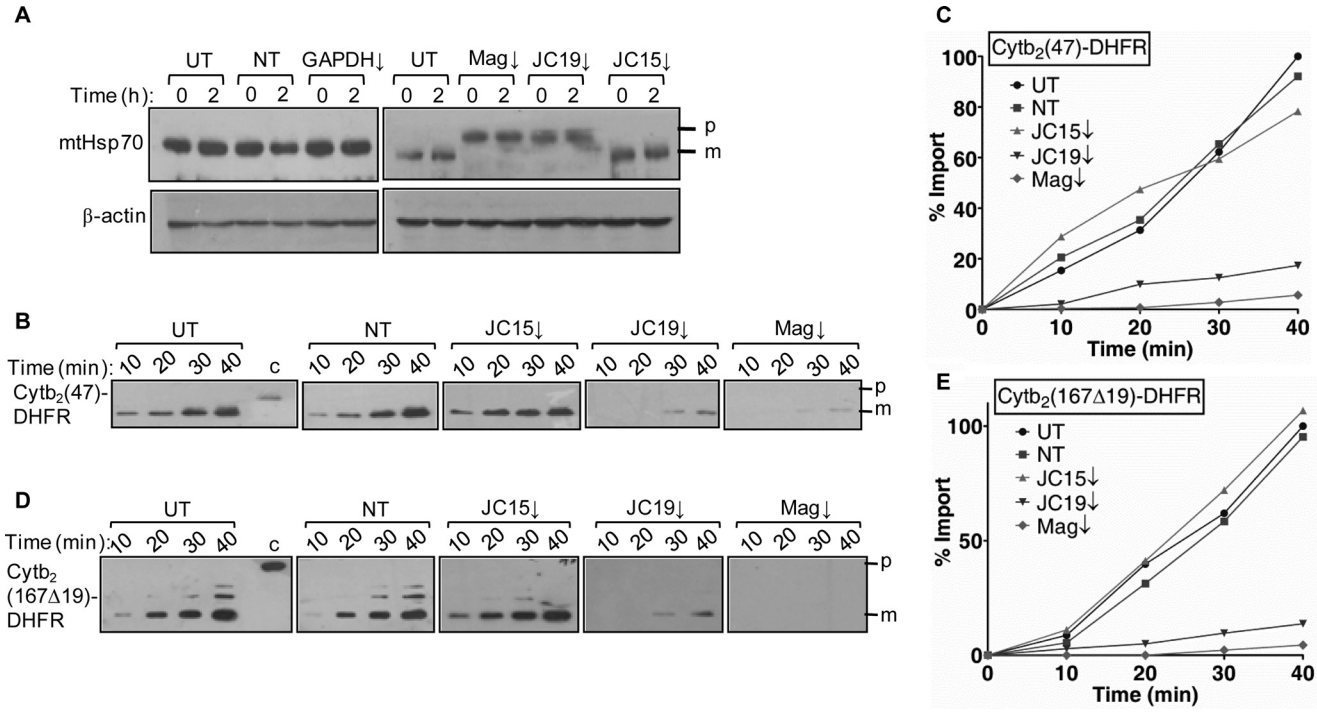

FIGURE 3. **Essentiality of J-proteins for protein translocation across the mitochondrial inner membrane.** *A*, HEK293T cells subjected to siRNA mediated down-regulation of Magmas (*Mag*), JC19, and JC15 were exposed to heat stress for 2 h at 45 °C. The cells were lysed in radioimmune precipitation assay buffer and probed for accumulation of the cytosolic precursor form and mitochondrial distribution of model protein mtHsp70; *p*, precursor; *m*, mature form. *B*, *C*, *D*, and *E*, the effect of J-protein knockdown on the import kinetics was monitored using two different matrix-targeted model precursor substrates, namely $Cytb_2$(47)-DHFR and $Cytb_2$(167Δ19)-DHFR (*p*). The amount of imported proteins was detected using anti-DHFR antibody (*m*) and quantified by densitometry and represented as a line graph (*C* and *E*). The amount of imported precursor for unsilenced (*UT*) mitochondria for the maximum import time was set to 100% (*UT*, untransfected control; *NT*, transfected with non-targeting dsiRNA as internal control; ↓, mRNA down-regulated by dsiRNA.

chondria (Fig. 2*C*) and total mitochondrial volume (Fig. 2*D*) as adjudged by MitoTracker Deep Red and *n*-nonyl acridine orange (NAO) staining, respectively. Comparatively, depletion of JC15 showed a marginal decrease in total mitochondrial content and active mitochondria than that of the unsilenced control (Fig. 2, *C* and *D*). Non-targeting RNA-transfected cells served as the negative control.

Because Magmas, JC19, and JC15 form a part of the mitochondrial protein transport complex, we assessed whether reduced mitochondria biogenesis is due to improper translocation of proteins into the organelle. We found that depleted Magmas and JC19 resulted in protein import defect, as demonstrated by accumulation of presequence-containing unprocessed forms of mitochondrial protein mtHsp70 (Fig. 3*A*). However, JC15-depleted cells did not show a significant defect in protein import across the inner membrane, co-relating with minimal changes in the levels of functional mitochondria (Fig. 3*A*). This shows that Magmas and JC19 play a critical role in translocation of precursor proteins in human mitochondria in normal cells, whereas JC15 has a dispensable function in protein import and cannot complement the protein translocation activity of JC19.

To further ascertain the importance of J-protein expression on protein translocation, we checked the effect of reduced expression of J-proteins on the import rate in isolated mitochondria. Mitochondria expressing lower levels of Magmas and JC19 showed reduced import kinetics for matrix-targeted $Cytb_2$(47)-DHFR and $Cytb_2$(167Δ19)-DHFR preproteins (Fig. 3, *B* and *C*, and Fig. 3, *D* and *E*). Consistent with the non-accumulation of precursor form of Hsp70, JC15 knockdown mitochondria did not show any detectable change in the rate of import of both the matrix-targeted preproteins (Fig. 3, *B*–*E*). These findings firmly establish the dispensable nature of JC15 at the translocase, whereas JC19 performs essential protein import function at translocase along with Magmas.

Human J-protein Orthologs, JC19 and JC15, Interact with Magmas with Similar Affinity—In contrast to the yeast system, our findings clearly suggest the existence of two J-protein subcomplexes in the human mitochondrial inner membrane translocation channel, having contrasting roles in maintenance of mitochondrial function. Because J-proteins function as a heterodimeric subcomplex with J-like protein to stimulate mtHsp70 ATPase activity in a regulated manner, it is likely possible that the functional diversity exhibited by these subcomplexes might be overall governed by their relative affinity of interaction at the translocation channel. The binding affinity between Magmas·JC19 and Magmas·JC15 was determined through two approaches, a semiquantitative GST pulldown approach and quantitative surface plasmon resonance. In the first approach, a comparative *in vitro* binding analysis through GST pulldown, was performed by incubating increasing concentrations of JC15 or JC19 purified proteins with GST-immobilized Magmas. Equivalent amounts of pulldown were observed for both JC19 and JC15, indicating that both JC19 and JC15 interact with Magmas with equal affinity (Fig. 4, *A* and *B*).

In the next approach we determined the dissociation constants of J-proteins for their interaction with Magmas through

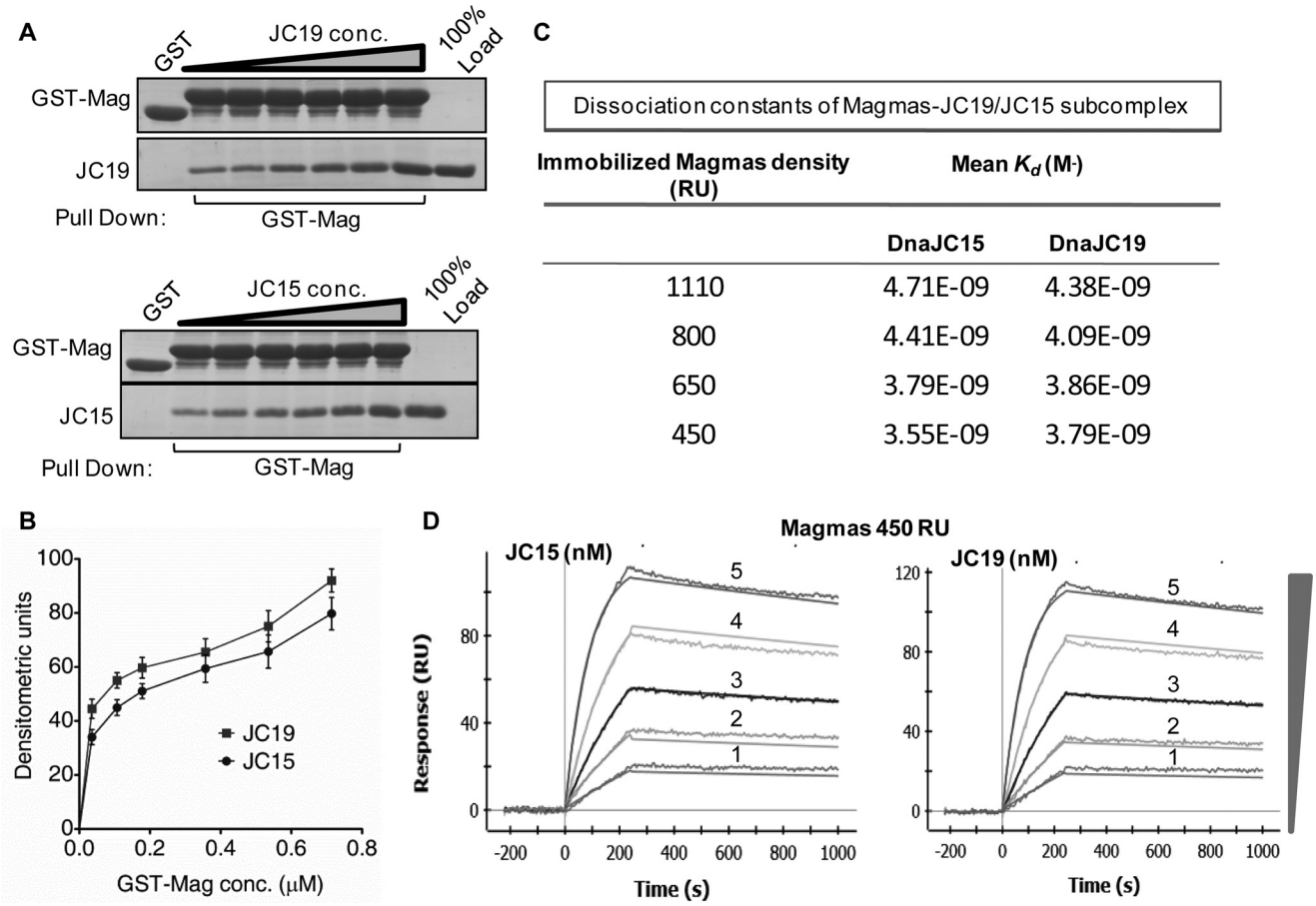

FIGURE 4. **Nature of subcomplex formation between JC15 and JC19 with Magmas.** *A* and *B*, immobilized GST-Magmas was incubated with increasing concentrations of either His_6-tagged JC19 or JC15 followed by SDS-PAGE analysis. The interacting proteins were visualized by Coomassie Blue staining. The bands were quantified by densitometry and plotted against a function of concentration (*B*) in the form of a *line graph*. GST alone was used as the negative control, and 100% input of the purified proteins was used as the loading control. *C*, table depicting dissociation constants (K_d) of Magmas·JC19 or Magmas·JC15 subcomplexes for different densities of Magmas immobilization titrated against increasing concentrations of JC15 and JC19 as mentioned in *D*. *D*, representative dissociation curve of surface plasmon resonance measurement upon increasing concentrations (19 nM, 38 nM, 75 nM, 150 nM, 300 nM) of JC19 or JC15 injected over immobilized Magmas at 450 response units (*RU*).

surface plasmon resonance over a range of concentrations. Increasing concentrations of JC19 or JC15 were injected over immobilized Magmas, and the relative dissociation constants were calculated. The mean K_d values revealed that both JC19 and JC15 form a subcomplex with Magmas with equal affinity (K_d = 3.55 ± 0.29 nM and 3.79 ± 0.19 nM, respectively) (Fig. 4, *C* and *D*). Similar results were obtained when binding analysis was done using variable concentrations of JC15 and JC19 over Magmas immobilized at different response units (K_d = 3.55 ± 0.29 − 4.71 ± 0.22 nM for JC15 and K_d = 3.79 ± 0.19 − 4.38 ± 0.48 nM for JC19 over the range of immobilized Magmas amounts) (supplemental Fig. S2). In summary, the results indicated that both JC19 and JC15 have equal affinity of interaction for Magmas.

JC15 and JC19 Possess Comparable Ability to Stimulate mtHsp70 ATPase Activity—The basal ATPase activity of mtHsp70 is insufficient to maintain a normal import process by itself (27, 28). Hence, J-proteins, Pam18 in yeast and JC19 in humans, play a critical role in catalytically stimulating the basal ATPase activity of mtHsp70 (23, 27, 28). The ATPase stimulatory activity of J-proteins is, however, inhibited by J-like proteins Pam16 or Magmas through formation of a subcomplex (11). Thus, a regulated stimulation of mtHsp70 ATPase activity is critical for driving the optimum import activity. Because human mitochondria consist of two J-proteins, JC15 and JC19, we analyzed their relative ability to stimulate human mtHsp70 ATPase activity and regulation by Magmas. To assess the activities, equivalent amounts of JC15 and JC19 were incubated with the preformed radioactive ATP·mtHsp70 complex, and the rate of conversion of ATP to ADP was measured under single turnover conditions. The amount of ADP was quantified to calculate the K_{cat} and represented as -fold stimulation over basal activity. We observed that at similar concentrations, both JC15 and JC19 stimulated mtHsp70's ATPase activity to equivalent levels (~3-fold) (Fig. 5*A*). The comparative inhibition of J-proteins' ATP stimulatory activity by Magmas was assessed by incubating equivalent ratios of Magmas·JC19 and Magmas·JC15 with radioactive ATP·Mortalin complex. Both the subcomplexes showed a similar -fold of inhibition (~60%) in stimulating Mortalin's ATPase activity (Fig. 5*A*). This indicates that Magmas regulates the activities of both the J-proteins by equivalent levels, and both JC15 and JC19 are competent to perform normal import function at the import channel.

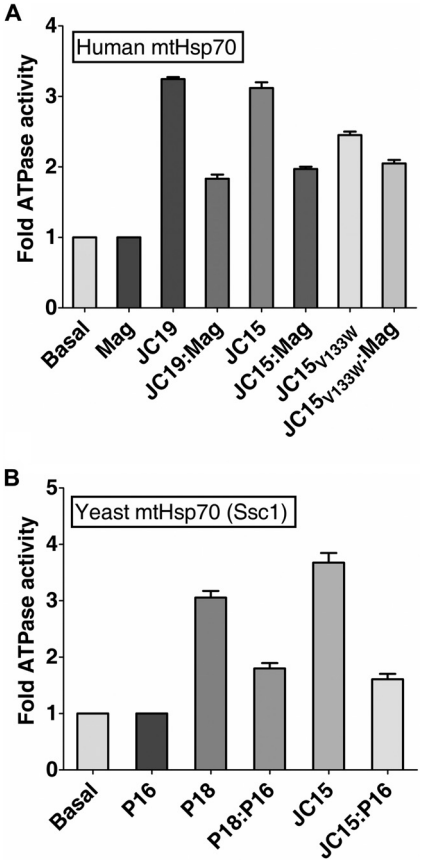

FIGURE 5. **Relative ability of the J-proteins to stimulate mtHsp70 ATPase activity.** *A*, comparative analysis of stimulation of human mtHsp70 ATPase activity by J-protein paralogs. mtHsp70·[α-^{32}P]ATP complex was incubated with a 2-fold excess of either Magmas (*Mag*) alone, JC19 alone, Magmas·JC19 subcomplex, JC15 alone, or Magmas·JC15 subcomplex, and the rate of hydrolysis was measured as the function of time at 23 °C. The basal rate of ATP hydrolysis by mtHsp70 alone was set to 1. The rate of conversion to ADP was measured and represented as -fold stimulation over the basal rate. $n = 3$, p (two tailed) < 0.001). *B*, effect of Pam16·JC15 subcomplex on Ssc1 ATPase activity. Ssc1·[α-^{32}P]ATP complex was incubated with a 2-fold excess of either Pam16 (*P16*) alone, JC15 alone, or Pam16·JC15 subcomplex, and the rate of hydrolysis was measured as a function of time at 23 °C. Pam18 (*P18*) was used as a positive control. The basal rate of ATP hydrolysis by Ssc1 alone was set to 1.

Because JC15 could rescue the growth Δ*pam18* yeast cells (25), we assessed whether the function of JC15 at the import channel is conserved, and it can simulate the basal ATPase activity of Ssc1 (yeast mtHsp70). Preformed radioactive Ssc1·[α-^{32}P]ATP complex was incubated with different molar ratios of purified proteins, and stimulation of Ssc1's ATPase activity was monitored under single turnover conditions. We observed an ~3.5-fold stimulation of Ssc1 ATPase activity by JC15, which is comparable with that of internal control Pam18 activity (Fig. 5*B*). Pam18·Pam16 subcomplex retained ~60% of the stimulatory activity of Pam18 alone over a range of complex concentrations. Similarly, JC15·Pam16 subcomplex showed ~50–60% activity in stimulating Ssc1 ATPase activity (Fig. 5*B*). This shows that human Pam18 orthologs function via a similar mechanism in governing the import process.

Conserved J-domain Function of Human and Yeast Pam18 Orthologs—The conserved functionality of JC15 and its yeast ortholog Pam18 was further co-related by altering the J-domain of JC15. Amino acid substitution of leucine at 150th position to tryptophan in Pam18 is associated with poor growth of cells and import defect (20). We substituted the corresponding residue in JC15, valine 133 to tryptophan. The mutant protein was purified and tested for its ability to stimulate the ATPase activity of Mortalin. Compared with wild type, $JC15_{V133W}$ alone showed a slightly lower stimulation of ATP hydrolysis rate of Mortalin; however, no substantial reduction in ATPase stimulatory activity was observed in the case of mutant JC15·Magmas subcomplex (Fig. 5*A*).

Because, JC15 and Magmas forms a stable subcomplex, we assessed whether the loss of regulation of ATP stimulatory activity of mutant JC15 is due to impaired subcomplex formation using GST pulldown analysis. The assay conducted using N-terminal truncations of the respective proteins having the J-domain and mitochondrial targeting region (J+T) or the J-domain alone (J), as the J-proteins are known to form a subcomplex through their putative J-domain (23). The pulldown analysis utilizing the mutant JC15 along with GST-Magmas J+T or GST-Pam16 J+T revealed that $JC15_{V133W}$ was unable to form a stable subcomplex with Magmas/Pam16 compared with its wild type counterpart (Fig. 6, *A* and *B*). However, the wild type JC15 J+T and J-fragments were able to associate comparably with respective Magmas fragments (Fig. 6, *C–E*). This shows that, like yeast Pam18 and human JC19 at the PAM complex, JC15 also associates with the translocase via its J-domain, with Val-133 playing a critical role.

The association of JC15 in a conserved manner with the transport machinery was further established with the isolation of the canonical ~250-kDa TIM23 complex in yeast mitochondria expressing JC15 (supplemental Fig. S3). Co-IP of JC15 along with Pam16 upon incubation of Triton X-100-lysed yeast mitochondria with anti-Pam16 beads showed formation of a stable JC15·Pam16 subcomplex (Fig. 6*F*). This association was, however, absent in $JC15_{V133W}$ yeast mitochondrial extracts, highlighting the conservation of this residue in subcomplex formation across kingdoms (Fig. 6*F*). The criticality and conserved nature of Val-133 residue in JC15's association with the presequence translocase was tested by co-IP of 1% digitonin-lysed yeast mitochondria using anti-Tim23 beads. Although immunoprecipitation of JC15 and internal control Pam18 along with other translocon components was observed in wild type, reduced immunoprecipitates of JC15 were present in mutant mitochondria (Fig. 6*G*). This clearly shows that JC15 follows a similar mechanism of association with the presequence translocase through Pam16.

To study whether the biochemical defects associated with $JC15_{V133W}$ result into a growth phenotype, we expressed the mutant in Δ*pam18* yeast cells. The $jc15_{V133W}$ cells grew slowly at 30 °C permissive temperature and were inviable at non-permissive temperatures of 34 °C and 37 °C (Fig. 7*A*). No changes in the expression level of the mutant protein and its association with mitochondrial inner membrane were observed (Fig. 7, *B* and *C*), implying a direct correlation between the poor growth of cells and interaction defects.

We next determined the ability of wild type and mutant JC15 to maintain mitochondrial specific organellar functions, including its biogenesis, by staining the logarithmically growing yeast cells by MitoTracker Deep Red and 10-*n*-nonyl acridine

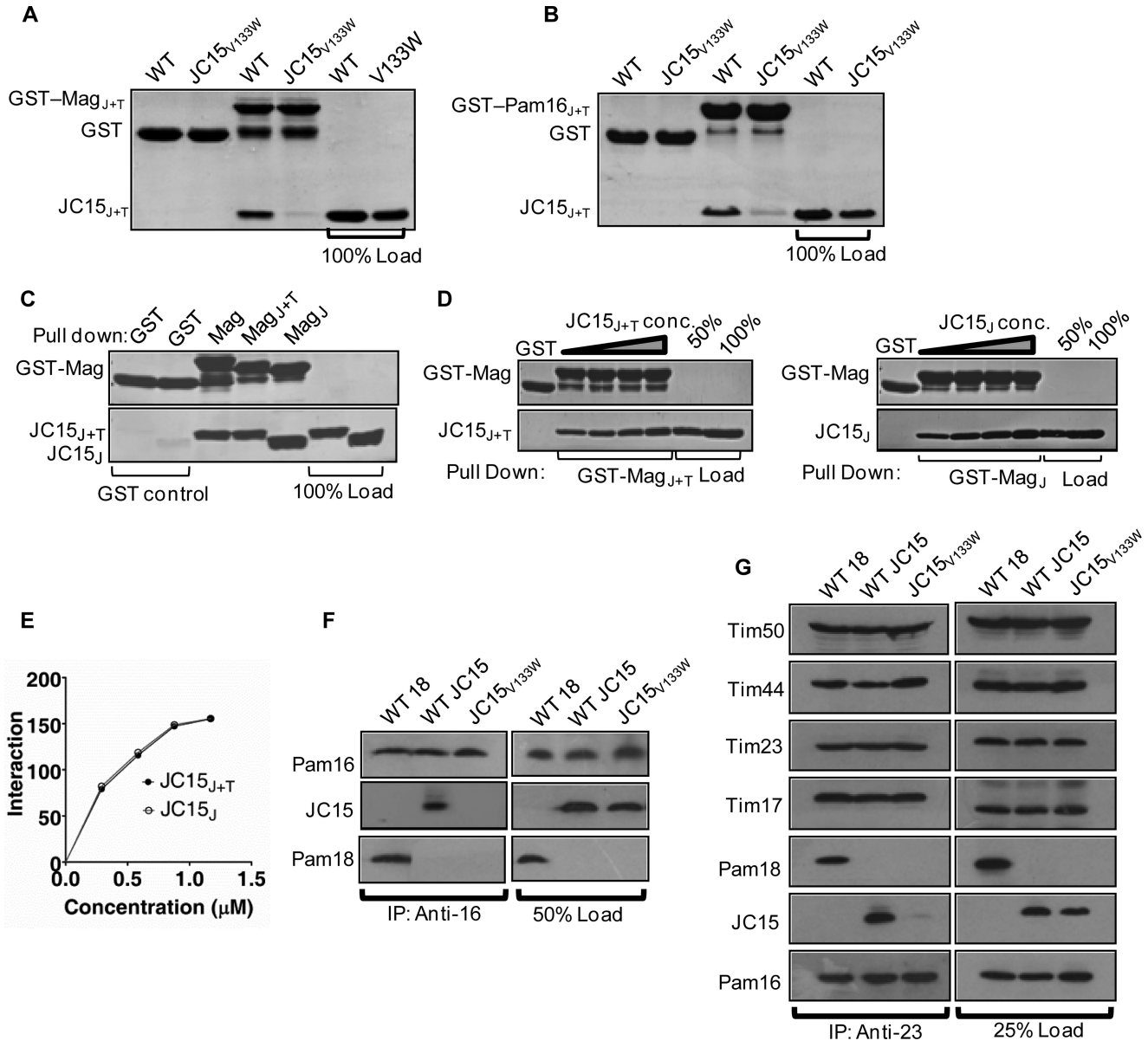

FIGURE 6. **JC15 forms a stable subcomplex with Pam16 to associate with the TIM23 complex.** *A* and *B*, subcomplex formation between JC15 mutant V133W and Magmas (*Mag*) (*A*) or Pam16 (*B*) was assayed by GST pulldown analysis where equimolar concentrations of wild type JC15 and $JC15_{V133W}$ mutant were incubated with immobilized GST-Magmas or GST-Pam16 fragments. The samples were separated on SDS-PAGE and analyzed by Coomassie Blue staining. 100% of wild type and mutant protein offered to the beads were loaded as loading control. GST-only conjugated beads were assayed as negative control. *C*, *D*, and *E*, equimolar (*C*) or increasing (*D*) concentrations of His_6-tagged $JC15_{J+T}$ and $JC15_J$ fragments were incubated with immobilized GST-$Magmas_{J+T}$ and GST-$Magmas_J$, respectively. The bound proteins were washed and analyzed by SDS-PAGE followed by Coomassie Blue staining. The bands were quantified by densitometry and represented as a line graph (*E*). Beads bound to GST-only were used as negative control. 50% or 100% input of the respective His_6-tagged proteins was used as loading control. *F*, mitochondria isolated from yeast cells expressing wild type Pam18, JC15, or $jc15_{V133W}$ mutant was subjected to lysis in buffer containing 1% Triton X-100 followed by incubation with anti-Pam16 antibody cross-linked beads. Samples were separated on SDS-PAGE and immunodecorated with antibodies specific to Pam16, JC15, and Pam18. 50% of the mitochondrial lysate was loaded as loading control (*50% Load*). *G*, interaction of JC15 with TIM23·core complex in yeast. Mitochondria from wild type and mutant yeast cells were solubilized using 1% digitonin, and immunoprecipitation was performed using anti-Tim23 antibodies. Samples were resolved on SDS-PAGE and immunodecorated with antibodies specific to the translocon components.

orange (NAO) to measure the functional and overall mitochondria volume, respectively, followed by flow cytometry analysis. We observed that yeast cells expressing wild type Pam18 or JC15 were comparable, whereas $jc15_{V133W}$ showed an almost 4–5-fold decrease in the fluorescence intensity (Fig. 7, *D* and *E*), indicating that JC15 mutant cells harbored comparatively lower mitochondrial content than wild type cells. Lastly, we checked the maintenance of mitochondrial membrane potential by labeling the yeast cells with JC-1. JC-1 is a mitochondria-specific cationic dye that exhibits potential-dependent accumulation in mitochondria, indicated by a fluorescence emission shift from green (~525 nm) to red (~590 nm) whose ratio gives a measure of membrane potential. We found that Pam18 and JC15-expressing cells showed a significantly higher red/green fluorescence ratio compared with $jc15_{V133W}$ cells, indicating the existence of unaltered membrane potential in wild types and loss of potential in case of the mutant (Fig. 7*F*). Together, these results suggest that JC15 restores bio-

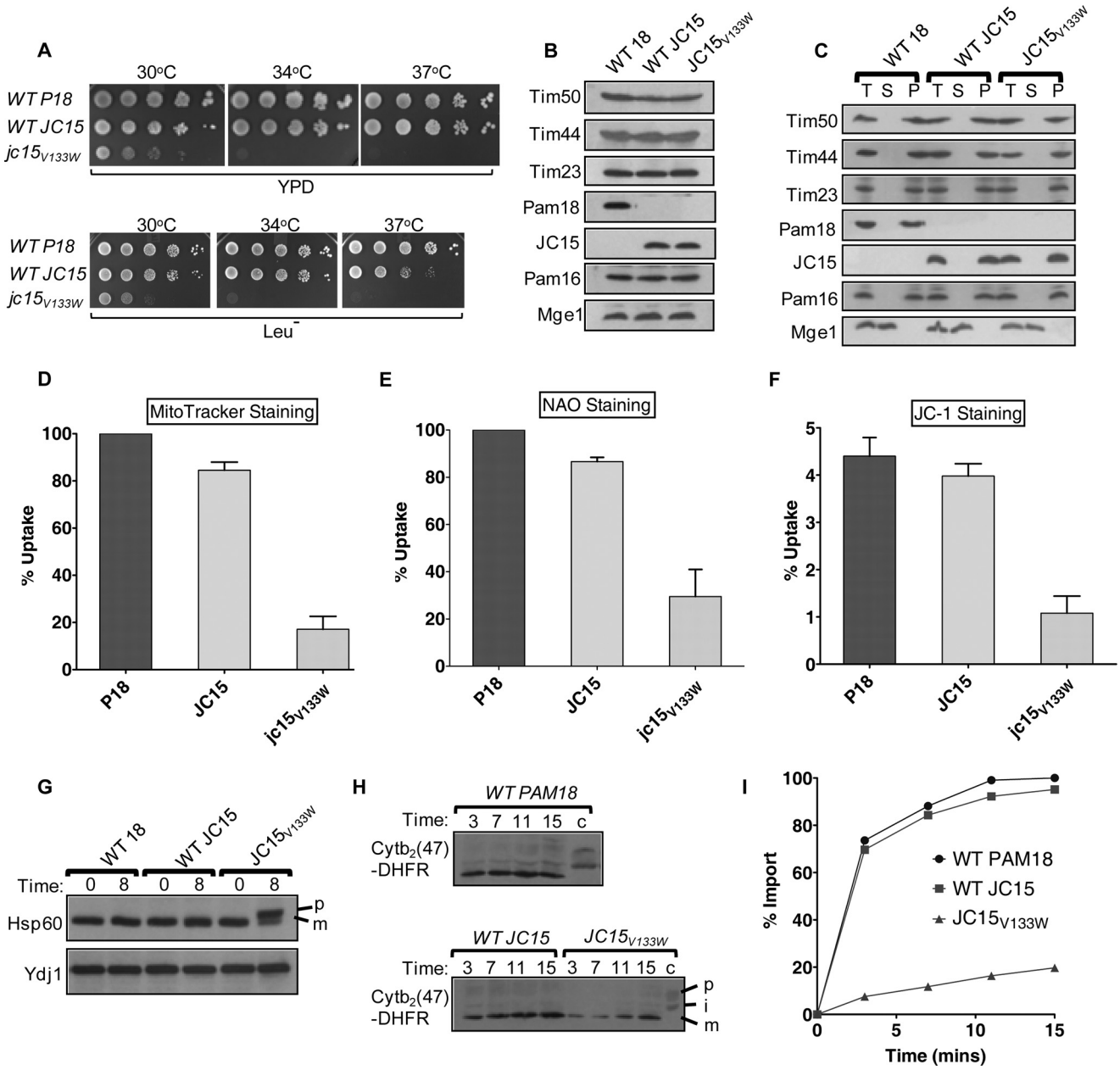

FIGURE 7. **J-domain mutation of JC15 results in a phenotype similar to Pam18.** *A*, 10-fold serial dilutions of wild type and mutant cells were spotted onto yeast extract/peptone/dextrose And Leucine drop out media (Leu^-) followed by incubation at the indicated temperatures for 48 h. *B*, expression analysis of TIM23 translocase components in the mutant. Equivalent amounts of wild type and mutant mitochondria were analyzed by SDS-PAGE and immunoblotting using specific antibodies against the translocon members. *C*, membrane association analysis of JC15 mutant. Mitochondria from wild type and mutant cells were sonicated, and the membrane fraction was separated by ultracentrifugation before electrophoresis. Unfractionated extract (*T*), soluble supernatant (*S*) and membrane pellet (*P*) fractions were immunoblotted using the indicated antibodies to determine the distribution of the respective proteins. *D*, *E*, and *F*, JC15 is critical for mitochondria biogenesis. Yeast cells expressing wild type Pam18, JC15, or JC15 mutant were stained by MitoTracker (*D*), NAO (*E*), or JC-1 (*F*) and subjected to flow cytometry measurements. The amount of dye uptake in case of wild type Pam18 cells was set at 100%. For JC-1 dye, the ratio of JC-1 red to green florescence was calculated and is represented as a *bar chart*. Valinomycin was used as positive control. Data are represented as $n = 3$, mean ± S.E. **, p (two tailed) < 0.001; ***, p (two tailed) < 0.0001. *G*, import of precursor proteins in JC15 mutant. Early log phase cultures of wild type and mutant JC15 yeast cells were subjected to heat shock at 37 °C for 8 h, and cell lysates were analyzed by SDS-PAGE and immunoblotted using specific anti-Hsp60 antibodies; *p*, precursor form; *m*, mature form of Hsp60. *H* and *I*, $Cytb_2(47)$-DHFR preprotein was imported into wild type or mutant mitochondria at 25 °C for the indicated time points. Reaction mixes were separated on SDS-PAGE and analyzed by immunoblotting and densitometry (*I*); *p*, precursor; *i*, intermediate; *m*, mature. The amount of m-$Cytb_2(47)$-DHFR in wild type Pam18 mitochondria after the longest import time was set to 100%.

genesis of mitochondria in Δ*pam18* yeast cells, which is mediated by its J-domain.

Therefore, to determine the role of JC15 in protein transport across the mitochondrial inner membrane *in vivo*, import of a model mitochondrial protein Hsp60 was analyzed. Upon subjecting the wild type Pam18 and JC15 yeast cells to heat stress, an undetectable amount of precursor protein was accumulated (Fig. 7*G*); however, consistent with the temperature-sensitive growth phenotype, exposure of the $jc15_{V133W}$ yeast cells to heat stress resulted in significant accumulation of precursor form of Hsp60, highlighting the import defect associated with the mutant (Fig. 7*G*). The translocation of preproteins into the

yeast mitochondria was kinetically monitored by measuring the import of a purified recombinant protein $Cytb_2$(47)-DHFR. Wild type or mutant mitochondria pre-exposed to 37 °C temperature stress was incubated with saturating amounts of recombinant precursor protein. Wild type Pam18 and JC15 showed almost similar import kinetics as compared with $JC15_{V133W}$ mitochondria, which showed a substantial reduction in kinetics of import (Fig. 7, *H* and *I*). The overlapping properties of Pam18 and JC15 in protein transport indicate a primary role of JC15 in mitochondrial protein import.

Dual Function of JC15 in Protein Import and Alteration of Cellular Drug Response—It is evident from our analysis that JC15 is orthologous to yeast Pam18, primarily involved in protein import function. However, previous reports suggest an additional role of JC15 in development of *de novo* cellular resistance to antineoplastic agents such as cisplatin and modulation of its expression by hypermethylation of CpG islands (29–32). Based on this evidence, we assessed whether JC15 could elicit a chemomodulatory function besides its housekeeping role in protein import in yeast cell. Yeast cells are known to trigger apoptosis in response to xenobiotic insult due to evolutionary conservation of the core apoptotic machinery up to a certain extent (39–41). To address the question, we utilized the two differentially expressing yeast promoters, a weaker *ADH* and stronger *TEF*, to mimic JC15's variable expression observed in chemorefractory cells. The yeast cells expressing Pam18 were used as an internal control to determine the basal level of cisplatin sensitivity of wild type cells. The yeast cells were initially exposed to varying concentrations of cisplatin and were then allowed to recover on rich media. We observed that at 30 °C and 300 μM cisplatin concentration, yeast cells expressing JC15 under *TEF* promoter grew very slowly as compared with *ADH* promoter and wild type Pam18 cells (Fig. 8, *A*, *D*, and *E*). However, upon increasing the cisplatin concentration to 500 μM, both *ADH*-JC15 and *TEF*-JC15 had an equivalent growth phenotype, and the overall size of the colonies was much smaller than Pam18 control cells (Fig. 8, *A*, *D*, and *F*). Similar results were obtained by cytotoxicity assays where yeast cells with *TEF*-JC15 formed lesser number of colonies than *ADH*-JC15 and wild type Pam18 cells over a range of cisplatin concentrations (supplemental Fig. S4*A*). Immunoblot analysis revealed a 2-fold higher expression of JC15 under *TEF* as compared with *ADH* promoter (Fig. 8, *B* and *C*), resulting in the sensitive phenotype. To adjudge the mechanism of cell death, the cisplatin-treated cells were stained with apoptotic marker annexin V and propidium iodide. The cells overexpressing JC15 under *TEF* promoter showed comparatively enhanced staining of annexin V/propidium iodide as compared with cells with lower levels of JC15 or Pam18 yeast cells (Fig. 8*G*). In addition, Pam18 expressing yeast cells showed higher uptake of mitochondrial potential-sensitive MitoTracker dye than cells with elevated JC15 levels (Fig. 8*I*). This shows that JC15-overexpressing cells shows increased propensity to apoptosis and is associated with loss of mitochondrial inner membrane potential upon drug treatment. In summary, our results highlight the association of JC15 expression with increased cisplatin sensitivity in yeast cells. The increase in cisplatin concentration resulted in poorer growth of JC15 yeast cells but had no effect on viability of Pam18 cells, thus indicating that JC15 expression by itself resulted in enhanced drug sensitivity.

To identify the domain of JC15 that is involved in development of chemosensitivity, we exposed the JC15 mutant $jc15_{V133W}$ with an impaired J-domain function, to 300 μM cisplatin. We observed that $jc15_{V133W}$ rescued the poor growth phenotype of wild type *TEF*-JC15 expressing yeast cells (Fig. 8*H*). The mutant cells showed decreased sensitivity to cisplatin and could grow faster and form comparatively more colonies than wild type JC15 cells (Fig. 8, *J–K*, and supplemental Fig. 4*B*). This shows that the chemotherapeutic response of JC15 is mediated via its J-domain.

Discussion

In the present study we comparatively assessed the functional specificities of both the J-proteins in human mitochondria and showed JC15 to be a bifunctional protein, having roles both in protein transport and chemosensitivity. JC15 was documented as a protein whose epigenetic silencing regulates the response to chemotherapeutic drug treatment and in normal cells of epithelial origin (30, 32, 42), whereas JC19 was identified as a protein whose mutation was associated with development of DCM syndrome (24). However, both JC19 and JC15 form a stable heterodimer with that of Magmas through their J-domain with equal affinity, which like other membrane-associated J-proteins, is the minimal region required for the interaction.

The protein translocation activity in mitochondria requires efficient chaperoning activity of mtHsp70 to vectorially pull the incoming polypeptide into the matrix (7, 14). The protein translocation function, being an ATP-dependent process, requires optimum ATPase activity of mtHsp70, which is stimulated by the J-protein counterpart Pam18 in the case of yeast. Loss of Pam18 function has been shown to be lethal for the yeast cell (27). The ability of JC15 to complement Pam18 function in yeast by rescuing the viability of Δ*pam18* cells and efficiently importing the precursor proteins is probably due to their higher sequence complementarity and similar domain organization, thus suggesting that JC15 was evolutionary more closely related to Pam18 than JC19 which lacks the ability to rescue Δ*pam18* cells (25). This is also supported by the fact that JC15 could stably interact with Pam16, form a part of TIM23 complex, and efficiently stimulate mtHsp70 ATPase activity. Loss of function mutations in the JC15 J-domain compromises its association with the translocon due to disruption of the subcomplex formation with Pam16 and causes dysregulation of import motor activity. This results in severe growth defects and translocation phenotypes, thereby affecting mitochondrial function and biogenesis.

In contrast to yeast, where there is a single J-protein Pam18 that is associated with the TIM23 complex (21), humans present a unique case of having two J-proteins, namely JC19 and JC15, as a part of the inner membrane translocation machineries (Fig. 9). Both the J-protein paralogs form two mutually distinct and functionally independent subcomplexes with their common J-like protein counterpart Magmas (Fig. 9). However, the majority of the protein transport processes are regulated by JC19, thereby playing a determining role in human mitochon-

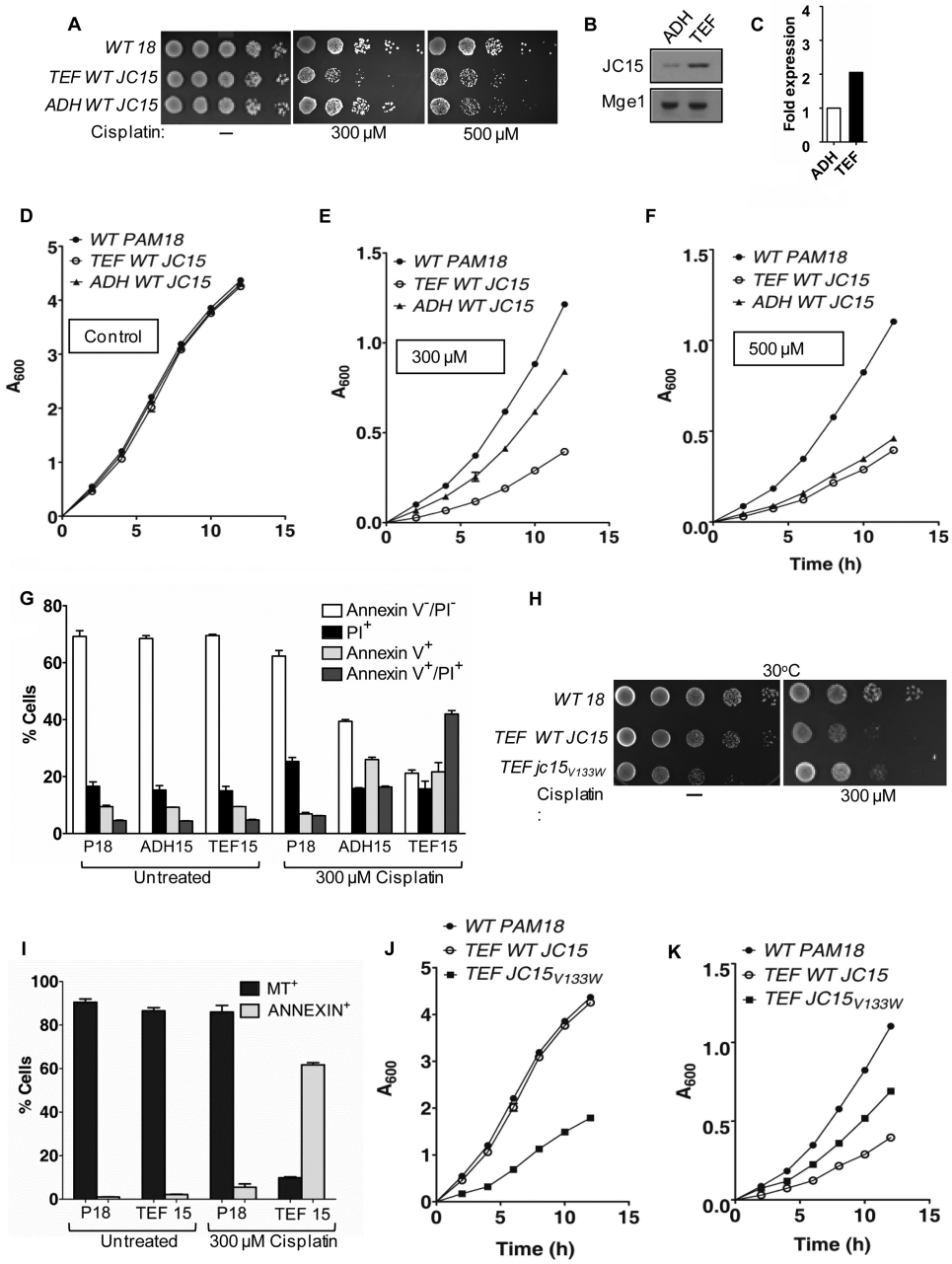

FIGURE 8. **Modulation of cellular response to cisplatin by JC15.** *A*, yeast cells expressing wild type Pam18 or JC15 were exposed to 300 μM or 500 μM cisplatin, and drop dilution analysis was performed on rich media. The plates were incubated at 30 °C for 48 h. *B*, expression immunoblot of yeast cells expressing JC15 under *TEF* or *ADH* promoter. Mge1 was used as loading control. *C*, the immunodecorated bands were quantified and are represented as -fold expression in the form of a *bar chart*. The densitometric unit of *ADH*-JC15 was set to 1. *D*, *E*, and *F*, growth curve analysis of yeast cells exposed to 300 μM or 500 μM cisplatin and incubated at 30 °C for indicated time periods. *G*, induction of apoptotic cell death by JC15. Yeast cells were left untreated or treated with 300 μM cisplatin before staining with annexin V and propidium iodide (*PI*) to label the apoptotic cell population. The relative number of cells positive for the dyes was represented as percent cells over the total analyzed cell population. The *bar* represents the mean ± S.E. $n = 3$; p (two tailed) < 0.001. *H*, wild type and mutant cells were exposed to 300 μM cisplatin and subjected to drop test analysis on yeast extract/peptone/dextrose followed by incubation at 30 °C for 48 h. *I*, yeast cells left untreated or exposed to cisplatin were stained with annexin V and MitoTracker Red (*MT*) to identify apoptotic cells with loss of mitochondrial membrane potential. The number of cells positive for the dyes is represented as a percentage for the total cell population analyzed. *Bars* represent mean ± S.E. $n = 3$, p (two tailed) < 0.001. *J* and *K*, yeast cells were incubated untreated (*J*) or treated with 300 μM cisplatin (*K*), and the growth of cells were monitored at 30 °C.

dria biogenesis, in contrast to JC15 which has a variable tissue-specific expression (31). The presence of two J-proteins involved in functional heterodimer with Magmas at the import channel assumes importance due to the fact that both JC19 and JC15 are associated with contrasting cellular phenotype (24, 30). A heterozygous mutation at the C-terminal region of JC19 leads to the formation of shorter protein with a truncated J-domain. This results in a debilitating disorder dilated cardiomyopathy and ataxia syndrome (DCM). DCM patients show profound neurodegeneration, skeletal muscle wastage, cardiac disorders leading to ataxia, and early age mortality (24). On the other hand, apart from its supportive role in protein transport, JC15 is suggested to modulate the organization and activity of electron chain complexes, a function also attributed to Mag-

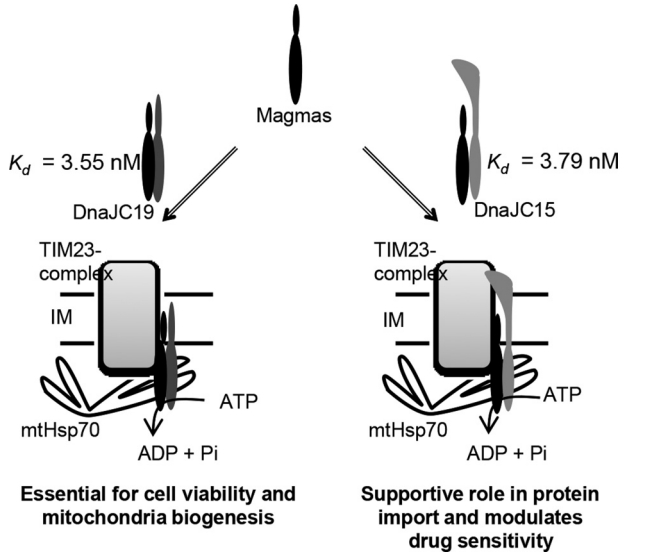

FIGURE 9. **Schematic representation of human J-protein paralogs at human mitochondrial import (*IM*) motor.** Comparative assessment of the biochemical properties of JC15 and JC19 for their association with the human TIM23 complex. *IM*, mitochondrial inner membrane.

mas, thus suggesting a possible role of JC15·Magmas subcomplex in regulation of respiratory activity (22, 34). Moreover, a specific loss of expression of JC15, especially in tissues of epithelial origin, results in development of chemoresistance against various chemotherapeutic drugs (30). Studies in cultured cells indicate stress-dependent association of JC15 with cyclophilin D in response to cisplatin treatment, which is responsible for recruitment of cyclophilin D to the mitochondrial transition pore complex, resulting in channel opening and induction of cell death (33). We found the chemomodulatory function of JC15 to be conserved across species, as yeast cells expressing the protein showed enhanced sensitivity to the drug. JC15 in addition to its complementation of the essential protein import function conferred increased drug sensitivity to yeast cells, highlighting its multifunctional role in the cell. The level of sensitivity was, however, proportional to the amount of protein expressed. Our results also highlight that the J-domain of JC15 plays a critical role in the overall process leading to development of the chemosensitive response.

The mitochondrial inner membrane J-proteins are thought to function in association with their corresponding J-like protein counterparts (18, 38, 43). Disruption of this heterodimeric subcomplex has been associated with loss of function and cellular lethality (20, 38). The contrasting functions of both the J-proteins paralogs, however, do not reflect on their properties at the translocase channel (Fig. 9). Both JC19 and JC15 have equal affinity of interaction with Magmas, stimulate human mtHsp70's activity to similar levels, and along with Magmas form higher order oligomeric structures unique to the mammalian system. Although a reduced level of JC15 is dispensable for cell survival and protein translocation, depletion of JC19 results in increased cell mortality, protein import defects, and decreased mitochondrial function, thus highlighting the inability to JC15 to complement JC19 function *in vivo*. This is consistent with clinical facts that DCM patients have a higher mortality rate with reduced life span, and the absence of JC15 expression is well tolerated by the cell as observed in normal fibroblasts and proliferating chemorefractory cancer cells (24, 30, 31). This indicates that the differential function of the two J-proteins in determining the cellular phenotype is independent of their individual association with the translocation channel and might be governed by the local primary sequence or secondary molecules, which are the focus of future investigations.

Experimental Procedures

Cells and Cell Culture—HEK293T, HeLa, HaCaT, IBR-3, OVCAR-3, and MCF7 cells were cultured in Dulbecco's modified Eagle's medium (DMEM) containing 10% fetal bovine serum and 1% penicillin-streptomycin at 37 °C in a humidified chamber containing 5% CO_2. LNCaP cells were grown in a RPMI 1640 medium under conditions mentioned above. Transfection of the cells with the siRNA was carried out using Lipofectamine 2000 (Invitrogen) as per the manufacturer's instructions and allowed to express for 48 h.

Plasmids, Yeast Strains, and Genetic Analysis—DNAJC15 was amplified from HeLa cell cDNA library using polymerase chain reaction and was subsequently cloned into the pRS415 yeast expression vector under *TEF* or *ADH* promoter. The temperature-sensitive yeast mutants for *DNAJC15* were obtained by generating a series of mutations in *pRS415 TEF-WTDNAJC15* through QuikChange site-directed mutagenesis protocol (Stratagene). The wild type and mutant clones were transformed into Δ*pam18* cells carrying *pRS316-WT PAM18* and were selected on leucine drop out plates. The transformants were streaked on 5-fluoroorotic acid plates to select the clones that supported growth of yeast cells at a permissible temperature but not at non-permissible temperatures. The temperature-sensitive mutant was rescued on rich media, and drop dilution analysis was performed to test the growth phenotype. All *in vivo* experiments were performed in yeast strains with W303 genetic background in derivatives of PJ53.

Full-length, J+T, and J-domain fragments of *DNAJC15* were hexahistidine-tagged at the N terminus and cloned between NdeI-BamHI sites in pET3a vector. GST fusion constructs of human Magmas J+T domain was generated by cloning the J+T fragment of Magmas at C-terminal of GST in pGEX-KG vector.

Mitochondrial Fractionation—For analysis of protein localization within mitochondria, fractionation of wild type and mutant mitochondria was essentially done as per published protocols (23). Briefly, mitochondria were subjected to hypotonic swelling in the sonication buffer followed by sonication at 30% duty per cycle. The supernatant and membrane pellet fraction were separated by ultracentrifugation at 90,000 × *g* for 1 h using Beckman Coulter Optima ultracentrifuge. The samples were separated on SDS-PAGE and subjected to immunoblot analysis using antibodies specific for either yeast or human mitochondrial proteins.

Determination of Mitochondria Biogenesis—Yeast cells expressing Pam18, wild type, or mutant JC15 were grown up to mid-log phase and exposed to heat shock at 37 °C for 5 h. The 4×10^5 cells were harvested and stained with 100 nM MitoTracker Deep Red to stain active mitochondria. Total mitochondrial volume was analyzed by staining with 5 μM of NAO.

Samples were analyzed by BD FACSCanto™ II, and the data were processed using BD FACSDiva software. The mean florescence indices were determined and plotted as percent dye uptake over the wild type. All the staining procedures were carried out for 30 min at 30 °C. Cellular autofluorescence was deducted before quantification of the dye uptake.

Co-Immunoprecipitation Analysis in Mitochondrial Lysates—The interactions between yPam16 and JC15 or Magmas, JC15, and JC19 were analyzed in yeast or human mitochondrial lysates, respectively, under the conditions where they have dissociated from the translocon. 2 mg of yeast or 500 μg of human mitochondria was subjected to lysis in the lysis buffer (20 mM MOPS-KOH, pH 7.4, 250 mM sucrose, 80 mM KCl, 5 mM EDTA, and 1 mM PMSF) in the presence of 1% Triton X-100 on ice for 45 min. Lysates were centrifuged for 15 min at 16,000 × *g* at 4 °C and incubated with a 20-μl bed volume of saturated Pam16 cross-linked antibody beads for 1 h at 4 °C. After subsequent washes in the lysis buffer, the samples were separated on SDS-PAGE followed by immunoblot analysis using specific antibodies.

Analysis of the association of JC15 with yeast translocon was done by solubilizing 2 mg of mitochondria in the lysis buffer (25 mM Tris, pH 7.5, 10% glycerol, 80 mM KCl, 5 mM EDTA, and 1 mM PMSF) in the presence of 1% digitonin at 4 °C for 50 min followed by centrifugation at 16,000 × *g* for 30 min at 4 °C. Supernatants were incubated with a 15-μl bed volume of saturated cross-linked yTim23 antibody beads for 2 h at 4 °C. Samples were washed in lysis buffer and resolved on SDS-PAGE. Immunoblotting was performed using antibodies specific to yeast translocon components.

RNAi Knockdown Experiments—HEK293T cells were seeded in Opti-MEM media (Invitrogen) and transfected with 5 μM dsiRNA duplexes pools; HSC.RNAI.N016069.12.1 and HSC.RNAI.N016069.12.2 (IDT) for *MAGMAS*; HSC.RNAI.N001190233.12.5 and HSC.RNAI.N001190233.12.7 (IDT) for *DNAJC19*; ON-TARGETplus SMART pool (Dharmacon) for *DNAJC15*. Transfection was performed using Lipofectamine 2000 (Invitrogen) according to the manufacturer's instructions.

Cell Viability and Cell Proliferation—The percentage of viable cells was determined by 3-(4,5-dimethylthiazol-2-yl)-2,5-diphenyltetrazolium bromide assay (MTT assay) (Invitrogen) as instructed in the manufacturer's manual. For cell cycle analysis, cells were fixed in 70% ethanol and RNase-treated followed by propidium iodide staining.

Protein Purification—For purification of J+T and J domains of JC15, a hexahistidine tag was introduced at the N terminus of the respective constructs and cloned into pET3a vector. Overexpression was carried out in BL21 strain of *Escherichia coli* at 30 °C. The wild type and mutant proteins were reconstituted from the insoluble fraction and purified using standard nickel-nitrilotriacetic acid affinity chromatography as previously described (23). The full-length GST-Magmas, GST-Magmas$_{J+T}$, and GST-Magmas$_{J}$ were purified according to the published protocols with minor modifications (23). The buffer components have been changed to 20 mM Tris, pH 7.5, instead of phosphate buffer in GST fusion protein purification protocols. Ssc1$_{His}$ was purified from yeast and human Mortalin from *E. coli* as described (37).

Protein Interaction Analysis—In vitro GST pulldown analysis using purified proteins was done essentially as described in previous protocols (23, 37). For surface plasmon resonance measurement, proteins were immobilized on GLC chip (Bio-Rad), and respective analytes were injected over the chip in phosphate-buffered saline, pH 7.4, containing 0.005% Tween 20 and 100 mM $MgCl_2$. Data analysis was done using Bio-Rad ProteOn™ XPR36 and fitted using Langmuir model.

In Vivo Import Assays—Wild type or altered mitochondria were preincubated in import buffer containing 2 mM ATP and 2 mM NADH followed by the addition of the precursor protein. The time of addition of the preprotein was noted as the zero time point, and accumulation of the precursor in the mitochondria was monitored over a fixed time scale. The reaction was stopped using valinomycin, and unimported preprotein was cleaved using proteinase K. The samples were separated on SDS-PAGE and immunoblotted using anti-DHFR-specific antibodies. The bands corresponding to the mature protein were quantified using ImageJ and plotted in form of a line graph. The maximum import to the wild type mitochondria was taken as 100%.

Yeast mitochondria were isolated according to published methods (14). The mutant mitochondria were preincubated at 37 °C before any kind of analysis. Expression analysis was carried out by subjecting 50 μg of yeast and 100 μg of human mitochondria to SDS-PAGE followed by immunoblotting using specific antibodies. Mitochondria were isolated from HEK293T cells grown in DMEM medium supplemented with 10% FBS using Cell Mitochondria Isolation Kit™ (Sigma) as per the manufacturer's instructions. Whole cell extracts were prepared in a radioimmune precipitation lysis buffer. Anti-JC15 antisera were generated by injecting the rabbits with purified J+T fragment of JC15 (Imgenx Biotech). The affinity purification of antibodies (21) and ATPase assays (27) were carried out as described. Immunoblot analysis was carried out by using the ECL system (Amersham Biosciences) according to the manufacturer's instructions.

Statistical Analysis—Calculation of statistical significance was done using two-tailed Student's *t* test through GraphPad Prism5 software unless otherwise mentioned; *p* values have been represented by comparing columns with WT and are mentioned in figure legends.

Author Contributions—D. S. and P. D. S. conceived the study and designed the experiments. D. S. performed the majority of the experiments. S. S. conducted experiments related to the growth phenotypes. All authors analyzed the data and wrote the manuscript.

Acknowledgments—We thank Prof. Elizabeth Craig for providing yeast strains and yeast-specific protein antibodies. We acknowledge the Bio-Rad Haifa facility, Israel, for performing surface plasmon resonance experiments. We thank the Flow Cytometry facility of Indian Institute of Science, Bangalore, for flow cytometry experiments.

References

1. Chan, D. C. (2006) Mitochondria: dynamic organelles in disease, aging, and development. *Cell* **125,** 1241–1252

2. Ernster, L., and Schatz, G. (1981) Mitochondria: a historical review. *J. Cell Biol.* **91,** 227s–255s
3. Neupert, W., and Herrmann, J. M. (2007) Translocation of proteins into mitochondria. *Annu. Rev. Biochem.* **76,** 723–749
4. Chacinska, A., Koehler, C. M., Milenkovic, D., Lithgow, T., and Pfanner, N. (2009) Importing mitochondrial proteins: machineries and mechanisms. *Cell* **138,** 628–644
5. Kamenskii, P. A., Vinogradova, E. N., Krasheninnikov, I. A., and Tarasov, I. A. (2007) [Directed import of macromolecules into mitochondria]. *Mol. Biol. (Mosk)* **41,** 216–233
6. Bolender, N., Sickmann, A., Wagner, R., Meisinger, C., and Pfanner, N. (2008) Multiple pathways for sorting mitochondrial precursor proteins. *EMBO Rep.* **9,** 42–49
7. Okamoto, K., Brinker, A., Paschen, S. A., Moarefi, I., Hayer-Hartl, M., Neupert, W., and Brunner, M. (2002) The protein import motor of mitochondria: a targeted molecular ratchet driving unfolding and translocation. *EMBO J.* **21,** 3659–3671
8. Voisine, C., Craig, E. A., Zufall, N., von Ahsen, O., Pfanner, N., and Voos, W. (1999) The protein import motor of mitochondria: unfolding and trapping of preproteins are distinct and separable functions of matrix Hsp70. *Cell* **97,** 565–574
9. Geissler, A., Chacinska, A., Truscott, K. N., Wiedemann, N., Brandner, K., Sickmann, A., Meyer, H. E., Meisinger, C., Pfanner, N., and Rehling, P. (2002) The mitochondrial presequence translocase: an essential role of Tim50 in directing preproteins to the import channel. *Cell* **111,** 507–518
10. Neupert, W., and Brunner, M. (2002) The protein import motor of mitochondria. *Nat. Rev. Mol. Cell Biol.* **3,** 555–565
11. Kampinga, H. H., and Craig, E. A. (2010) The HSP70 chaperone machinery: J proteins as drivers of functional specificity. *Nat. Rev. Mol. Cell Biol.* **11,** 579–592
12. Mokranjac, D., Sichting, M., Popov-Celeketić, D., Berg, A., Hell, K., and Neupert, W. (2005) The import motor of the yeast mitochondrial TIM23 preprotein translocase contains two different J proteins, Tim14 and Mdj2. *J. Biol. Chem.* **280,** 31608–31614
13. Kang, P. J., Ostermann, J., Shilling, J., Neupert, W., Craig, E. A., and Pfanner, N. (1990) Requirement for hsp70 in the mitochondrial matrix for translocation and folding of precursor proteins. *Nature* **348,** 137–143
14. Liu, Q., D'Silva, P., Walter, W., Marszalek, J., and Craig, E. A. (2003) Regulated cycling of mitochondrial Hsp70 at the protein import channel. *Science* **300,** 139–141
15. Bukau, B., Weissman, J., and Horwich, A. (2006) Molecular chaperones and protein quality control. *Cell* **125,** 443–451
16. Laufen, T., Mayer, M. P., Beisel, C., Klostermeier, D., Mogk, A., Reinstein, J., and Bukau, B. (1999) Mechanism of regulation of hsp70 chaperones by DnaJ cochaperones. *Proc. Natl. Acad. Sci. U.S.A.* **96,** 5452–5457
17. Misselwitz, B., Staeck, O., and Rapoport, T. A. (1998) J proteins catalytically activate Hsp70 molecules to trap a wide range of peptide sequences. *Mol. Cell* **2,** 593–603
18. Mokranjac, D., Berg, A., Adam, A., Neupert, W., and Hell, K. (2007) Association of the Tim14·Tim16 subcomplex with the TIM23 translocase is crucial for function of the mitochondrial protein import motor. *J. Biol. Chem.* **282,** 18037–18045
19. Mokranjac, D., Bourenkov, G., Hell, K., Neupert, W., and Groll, M. (2006) Structure and function of Tim14 and Tim16, the J and J-like components of the mitochondrial protein import motor. *EMBO J.* **25,** 4675–4685
20. D'Silva, P. R., Schilke, B., Hayashi, M., and Craig, E. A. (2008) Interaction of the J-protein heterodimer Pam18/Pam16 of the mitochondrial import motor with the translocon of the inner membrane. *Mol. Biol. Cell* **19,** 424–432
21. Kozany, C., Mokranjac, D., Sichting, M., Neupert, W., and Hell, K. (2004) The J domain-related cochaperone Tim16 is a constituent of the mitochondrial TIM23 preprotein translocase. *Nat. Struct Mol. Biol.* **11,** 234–241
22. Srivastava, S., Sinha, D., Saha, P. P., Marthala, H., and D'Silva, P. (2014) Magmas functions as a ROS regulator and provides cytoprotection against oxidative stress-mediated damages. *Cell Death Dis.* **5,** e1394
23. Sinha, D., Joshi, N., Chittoor, B., Samji, P., and D'Silva, P. (2010) Role of Magmas in protein transport and human mitochondria biogenesis. *Hum. Mol. Genet.* **19,** 1248–1262
24. Davey, K. M., Parboosingh, J. S., McLeod, D. R., Chan, A., Casey, R., Ferreira, P., Snyder, F. F., Bridge, P. J., and Bernier, F. P. (2006) Mutation of DNAJC19, a human homologue of yeast inner mitochondrial membrane co-chaperones, causes DCMA syndrome, a novel autosomal recessive Barth syndrome-like condition. *J. Med. Genet.* **43,** 385–393
25. Schusdziarra, C., Blamowska, M., Azem, A., and Hell, K. (2013) Methylation-controlled J-protein MCJ acts in the import of proteins into human mitochondria. *Hum. Mol. Genet* **22,** 1348–1357
26. Sinha, D., Srivastava, S., Krishna, L., and D'Silva, P. (2014) Unraveling the intricate organization of mammalian mitochondrial presequence translocases: existence of multiple translocases for maintenance of mitochondrial function. *Mol. Cell. Biol.* **34,** 1757–1775
27. D'Silva, P. D., Schilke, B., Walter, W., Andrew, A., and Craig, E. A. (2003) J protein cochaperone of the mitochondrial inner membrane required for protein import into the mitochondrial matrix. *Proc. Natl. Acad. Sci. U.S.A.* **100,** 13839–13844
28. Truscott, K. N., Voos, W., Frazier, A. E., Lind, M., Li, Y., Geissler, A., Dudek, J., Müller, H., Sickmann, A., Meyer, H. E., Meisinger, C., Guiard, B., Rehling, P., and Pfanner, N. (2003) A J-protein is an essential subunit of the presequence translocase-associated protein import motor of mitochondria. *J. Cell Biol.* **163,** 707–713
29. Lindsey, J. C., Lusher, M. E., Strathdee, G., Brown, R., Gilbertson, R. J., Bailey, S., Ellison, D. W., and Clifford, S. C. (2006) Epigenetic inactivation of MCJ (DNAJD1) in malignant paediatric brain tumours. *Int. J. Cancer* **118,** 346–352
30. Shridhar, V., Bible, K. C., Staub, J., Avula, R., Lee, Y. K., Kalli, K., Huang, H., Hartmann, L. C., Kaufmann, S. H., and Smith, D. I. (2001) Loss of expression of a new member of the DNAJ protein family confers resistance to chemotherapeutic agents used in the treatment of ovarian cancer. *Cancer Res.* **61,** 4258–4265
31. Strathdee, G., Davies, B. R., Vass, J. K., Siddiqui, N., and Brown, R. (2004) Cell type-specific methylation of an intronic CpG island controls expression of the MCJ gene. *Carcinogenesis* **25,** 693–701
32. Strathdee, G., Vass, J. K., Oien, K. A., Siddiqui, N., Curto-Garcia, J., and Brown, R. (2005) Demethylation of the MCJ gene in stage III/IV epithelial ovarian cancer and response to chemotherapy. *Gynecol. Oncol.* **97,** 898–903
33. Sinha, D., and D'Silva, P. (2014) Chaperoning mitochondrial permeability transition: regulation of transition pore complex by a J-protein, DnaJC15. *Cell Death Dis.* **5,** e1101
34. Hatle, K. M., Gummadidala, P., Navasa, N., Bernardo, E., Dodge, J., Silverstrim, B., Fortner, K., Burg, E., Suratt, B. T., Hammer, J., Radermacher, M., Taatjes, D. J., Thornton, T., Anguita, J., and Rincon, M. (2013) MCJ/DnaJC15, an endogenous mitochondrial repressor of the respiratory chain that controls metabolic alterations. *Mol. Cell. Biol.* **33,** 2302–2314
35. Ojala, T., Polinati, P., Manninen, T., Hiippala, A., Rajantie, J., Karikoski, R., Suomalainen, A., and Tyni, T. (2012) New mutation of mitochondrial DNAJC19 causing dilated and noncompaction cardiomyopathy, anemia, ataxia, and male genital anomalies. *Pediatr Res.* **72,** 432–437
36. Bauer, M. F., Gempel, K., Reichert, A. S., Rappold, G. A., Lichtner, P., Gerbitz, K. D., Neupert, W., Brunner, M., and Hofmann, S. (1999) Genetic and structural characterization of the human mitochondrial inner membrane translocase. *J. Mol. Biol.* **289,** 69–82
37. Goswami, A. V., Chittoor, B., and D'Silva, P. (2010) Understanding the functional interplay between mammalian mitochondrial Hsp70 chaperone machine components. *J. Biol. Chem.* **285,** 19472–19482
38. D'Silva, P. R., Schilke, B., Walter, W., and Craig, E. A. (2005) Role of Pam16's degenerate J domain in protein import across the mitochondrial inner membrane. *Proc. Natl. Acad. Sci. U.S.A.* **102,** 12419–12424
39. Carmona-Gutierrez, D., Eisenberg, T., Büttner, S., Meisinger, C., Kroemer, G., and Madeo, F. (2010) Apoptosis in yeast: triggers, pathways, subroutines. *Cell Death Differ* **17,** 763–773
40. Büttner, S., Eisenberg, T., Herker, E., Carmona-Gutierrez, D., Kroemer, G., and Madeo, F. (2006) Why yeast cells can undergo apoptosis: death in times of peace, love, and war. *J. Cell Biol.* **175,** 521–525

41. Madeo, F., Herker, E., Wissing, S., Jungwirth, H., Eisenberg, T., and Fröhlich, K. U. (2004) Apoptosis in yeast. *Curr. Opin. Microbiol* **7,** 655–660
42. Hatle, K. M., Neveu, W., Dienz, O., Rymarchyk, S., Barrantes, R., Hale, S., Farley, N., Lounsbury, K. M., Bond, J. P., Taatjes, D., and Rincón, M. (2007) Methylation-controlled J protein promotes c-Jun degradation to prevent ABCB1 transporter expression. *Mol. Cell. Biol.* **27,** 2952–2966
43. Frazier, A. E., Dudek, J., Guiard, B., Voos, W., Li, Y., Lind, M., Meisinger, C., Geissler, A., Sickmann, A., Meyer, H. E., Bilanchone, V., Cumsky, M. G., Truscott, K. N., Pfanner, N., and Rehling, P. (2004) Pam16 has an essential role in the mitochondrial protein import motor. *Nat. Struct. Mol. Biol.* **11,** 226–233